

Substituted AlPO_4 -11 molecular sieves—SAPO-11 and CoAPO-11: Synthesis, acidity and alkylation of toluene with methanol

J Das, S P Lohokare & D K Chakrabarty*

Solid State Laboratory, Chemistry Department, Indian Institute of Technology, Bombay 400 076, India
Received 21 October 1991; revised 17 December 1991; accepted 27 January 1992

AlPO_4 -11 as well as substituted SAPO-11 and CoAPO-11 have been synthesized hydrothermally in the pure state. Results of acidity measurement show that the acid strength depends on the substituent. This is also supported by the results of alkylation of toluene with methanol on these catalysts. These molecular sieves exhibit very high *para* selectivity because of the elliptical 10-membered oxygen ring channels.

Aluminium phosphate molecular sieves (AlPO_4s) have been gaining importance in recent years. They are made of alternating AlO_4 and PO_4 tetrahedra. One such structure, AlPO_4 -11 has 10-membered oxygen ring channels with diameter $6.3 \times 3.9 \text{ \AA}$, similar to that of medium pore zeolites¹. Although AlPO_4s have an electroneutral framework and possess only weak Bronsted acidity due to the presence of defects, substitution of aluminium and/or phosphorus by cations with lower charge introduces a negative charge in the frame. This is countered by protons imparting Bronsted acidity. Thus, substitution of silicon for phosphorus in the AlPO_4 -11 frame gives² acidic SAPO-11 and substitution of a number of divalent metal ions for aluminium gives³ acidic MeAPO. Presence of acid sites makes SAPOs and MeAPOs good catalysts for reactions of aromatics such as alkylation and disproportionation of toluene, isomerization and disproportionation of the xylenes, etc. Substituted AlPO_4 -11, however, has the additional advantage of restricted pore diameter over AlPO_4 -5, that can lead to shape selectivity. Thus, it was found⁴ that toluene undergoes selective alkylation by methanol on SAPO-11, whereas disproportionation and alkylation proceeds⁵ with equal ease on wide pore

SAPO-5. These differences arise essentially because of restricted transition state shape selectivity.

Co^{2+} is not likely to enter a phosphorus site and hence CoAPO is expected to have different acidity. In order to check the various concepts, we have synthesized SAPO-11 (with low and high silicon substitution) and CoAPO-11 and studied their acidity as well as the catalytic alkylation of toluene with methanol on them. The results are reported here.

Materials and Methods

Synthesis

Pseudoboehmite (catapol B) and Ludox AS-40 were used as source of alumina and silica respectively. The other chemicals used were orthophosphoric acid (85% AR), dipropylamine (DPA) and cobalt sulphate (AR). The composition of the synthesis mixture and the experimental conditions are given in Table 1.

Half of the required amount of water was added to pseudoboehmite and stirred vigorously to a slurry followed by the addition of orthophosphoric acid slowly with constant stirring. The remaining water was then added and stirring was continued for 2 hr after which DPA was added. After further 2 hr of

Table 1—Molar composition of the reaction mixture for preparation of AlPO_4 -11 and related structures and synthesis conditions

Sample	Al_2O_3	P_2O_5	SiO_2	H_2O	DPA	pH	Heating period (h)
AlPO_4 -11	1	1	0	40	1.0	3.40	24
SAPO-11/1	1	1	0.1	40	1.0	3.43	24
SAPO-11/4	1	1	0.4	40	1.0	3.46	96
CoAPO-11	1	1	0.1	40	1.0	3.41	24

vigorous stirring when the pH was stabilized at 3.4-3.5, the mixture was transferred to a stainless steel autoclave and heated at 200°C. For obtaining SAPO-11 and CoAPO-11, silica or cobalt source was added before DPA. The crystalline product was washed and dried at 100-110°C for 16 hr. The occluded DPA was removed by calcining at 520°C. SAPO-11/1 gave the chemical analysis corresponding to Al₂O₃ : SiO₂ : P₂O₅ as 1.0 : 0.07 : 0.94. The Al₂O₃ : SiO₂ : P₂O₅ ratio for SAPO-11/4 was 1.0 : 0.30 : 0.95.

X-ray diffraction and electron microscopy

X-ray powder diffraction patterns of the as-synthesized as well as calcined samples were recorded on a PW 1820 X-ray diffractometer using CuK_α radiation. SEM photographs at different magnifications were taken using a JEOL 6400 Scanning Electron Microscope.

UV-visible spectroscopy

UV-visible spectrum of CoAPO-11 was recorded on an Aminco DW-2a UV/Vis spectrophotometer in the reflectance mode using barium sulphate as reference.

Temperature programmed desorption of ammonia

Temperature programmed desorption of ammonia was recorded on an instrument assembled in the laboratory using a thermal conductivity detector. A heating rate, 10°C/min with helium as carrier gas was used. The spectra were resolved into gaussians using a computer program from which the number of ammonia molecules desorbed at various temperature were evaluated.

Catalytic conversion

Alkylation of toluene with methanol was studied in a down-flow glass reactor. The reactants were fed accurately by a peristaltic pump. The products were condensed by passing through a condenser and

finally, using an ice-salt bath and analysed by GC using FID detectors and a 4m long column packed with 5% diisodecylphthalate + 5% Benton on chromosorb (100-200 mesh).

Results and Discussion

Structure

XRD powder pattern of the as-synthesized CoAPO₄-11 is given in Fig. 1. The results are in very good agreement with the literature⁶ and do not indicate any variation in lattice size with substitution. Electron micrographs (Fig.2) showed large spherical agglomerates consisting of elongated crystals upto 1 μm wide and about 3 μm long. They are stacked to form large spherical aggregates. The UV-visible reflectance spectrum of CoAPO-11 is shown in Fig. 3. The intense blue colour of the sample and the typical visible spectrum of tetrahedral Co²⁺ with bands at 538, 580 and 626 nm confirm that cobalt has entered the framework⁷.

Acidity

Figure 4 shows the TPD of ammonia for the various samples. To avoid physisorption, adsorption of ammonia was carried out at 100°C and the desorption spectra were recorded at this temperature. The results

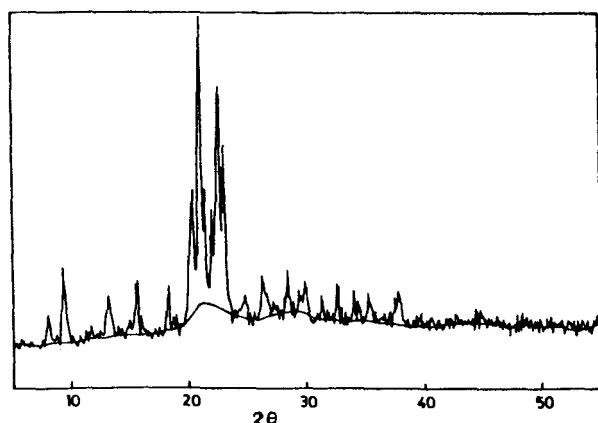


Fig.1—X-ray diffraction pattern of CoAPO-11 (as-synthesized).

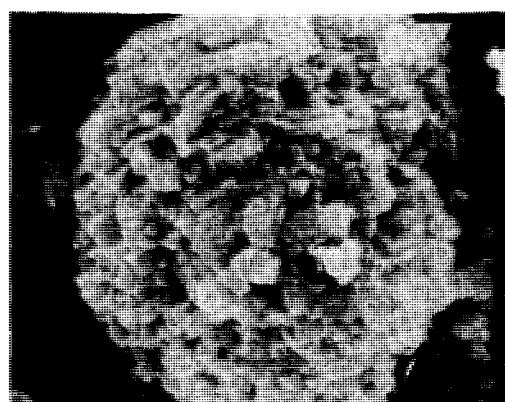
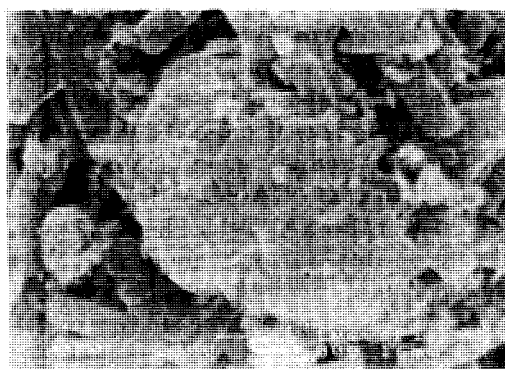


Fig. 2—Electron micrographs of as-synthesized samples [(a) SAPO-11/1 and (b) CoAPO-11].

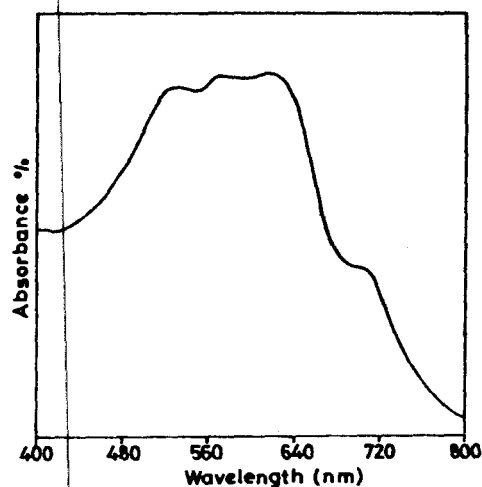


Fig. 3—UV-vis spectrum of CoAPO-11.

of acidity as obtained from the resolved gaussians are given in Table 2. SAPO-11 samples show two desorption maxima at 165°C (α) and 260°C (β) respectively. Compared to this, AlPO_4 -11 had only the weak acidic peak at 165°C, whereas CoAPO-11 had an additional high temperature peak at 370°C (γ). This shows that substitution of Co^{2+} in the AlPO_4 -11 framework generates stronger acid centres. Acidity of all these molecular sieves, however, is much weaker as compared to that of the medium pore zeolite⁸ ZSM-5. Acidity data of SAPO-5 have been included in Table 2 for comparison. The two samples, SAPO-5 and SAPO-11/1 synthesized from gel with similar Si:P ratio (1:20) showed large difference in total acidity. This proves that silicon incorporation at P sites is easier in case of AlPO_4 -5 framework. The synthesis mixture for SAPO-11/4 had Si:P ratio 1:5, but its total acidity was only about sixty per cent higher. Since total acidity will also include any surface silanol due to amorphous silica, it is better to compare the acid centres of medium strength (β peak) which increases only by 25 per cent in going from SAPO-11/1 to SAPO-11/4.

It has been recently shown by Jahn *et al.*⁹ that silicon can get incorporated into the AlPO_4 -11 framework through (i) a silicon atom entering into a P site or (ii) two silicon atoms entering as pair into one P and one Al sites. Martens *et al.*¹⁰, on the other hand, propose that higher amount of silicon substitution will lead to the formation of a SAPO domain and a zeolite domain. Acidity generated in a zeolite framework will be much stronger⁸ and such strong acid sites are absent in our samples. This would require that the extra silicon should substitute both aluminium and phosphorus in pairs, or it should remain as amorphous silica. In either case, it will have

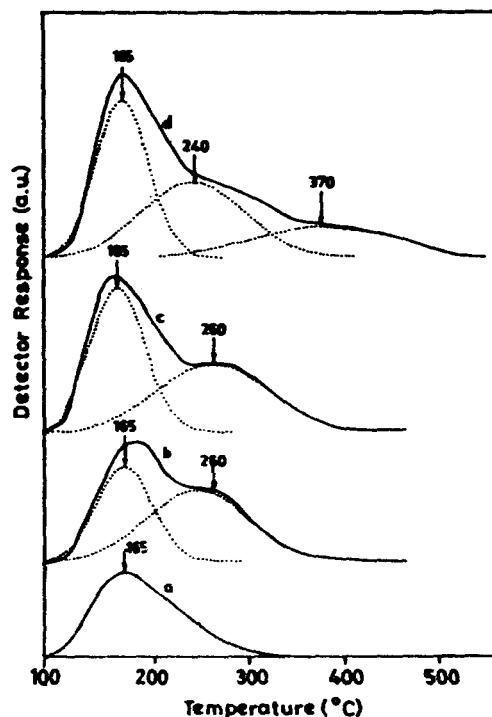
Fig. 4—Ammonia desorption profiles of (a) AlPO_4 -11; (b) SAPO-11/1; (c) SAPO-11/4; and (d) CoAPO-11.

Table 2—Acidity of the aluminium phosphate molecular sieves from ammonia desorption

Sample	Acidity (mmol of ammonia absorbed/g of sample)			
	Total	α (165°C)	β (~ 260°C)	γ (370°C)
SAPO-11/1	0.117	0.049	0.068	—
SAPO-11/4	0.187	0.100	0.087	—
AlPO_4 -11	0.105	0.105	—	—
CoAPO-11	0.190	0.074	0.076	0.040
SAPO-5	0.366	0.139	0.227	—

no effect on the framework charge. The presence of amorphous silica, however, will increase the intensity of the α -peak in the TPD profile which has actually been observed. It appears that silicon initially substitutes phosphorus, and at higher concentrations, either pair-wise substitution takes place, or the phase also has amorphous silica or both situations coexist. The results of chemical analysis show that SAPO-11/4 contains much higher amount of silicon, but most of it is not in the frame. However, further investigation is needed to establish this point. As compared to this, cobalt easily substitutes aluminium in AlPO_4 -11 as seen from the higher total acidity of CoAPO-11 as compared to that of SAPO-11/1 although both of them had the same

amount of the substituting atoms in the synthesis mixture.

Alkylation of toluene

Alkylation of toluene with methanol on SAPO-11 and CoAPO-11 gave the three xylenes and 1,2,4-trimethylbenzene (TMB). The catalysts deactivated rapidly with time (Fig. 5). Table 3 shows the product distribution for the various catalysts under identical experimental conditions at 30 min time on stream. Conversion was less than 1% on AlPO₄-11 whereas highest conversion took place on CoAPO-11. TPD shows that AlPO₄-11 has only weak acid sites (α peak) whereas CoAPO-11 has much stronger acid centres (β and γ). Therefore, it may be concluded that toluene conversion takes place at the moderately strong acid sites. The same conclusion is arrived at by comparing toluene conversion on SAPO-11/1 and SAPO-11/4. Although total acidity of SAPO-11/4 is much higher than that of SAPO-11/1, initial conversion on the former is only slightly higher because the relative concentration of the moderately strong acid sites (β)

is only 25% higher in SAPO-11/4. It can be seen that toluene conversion on SAPO-11/4 is about 20% higher than on SAPO-11/1 showing a close parallel between the concentration of moderately strong acid sites and catalytic activity. CoAPO-11, on the other hand, has a greater number of stronger acid centres (β and γ) and hence shows much higher initial conversion and also rapid deactivation due to coking.

Results of acidity as well as toluene conversion do not suggest the formation of a zeolite domain as proposed by Martens *et al.*¹⁰, at least in this composition range. If that was to happen, SAPO-11/4 would have shown much higher conversion of toluene than SAPO-11/1.

Table 3 also shows high *para* selectivity of these medium pore molecular sieves. *Para* selectivity of toluene methylation is generally considered as a clear case of product shape selectivity. The medium pore zeolite ZSM-5 is known to give a near equilibrium mixture of the xylenes¹¹ although large crystals give about 46% *para*-xylene¹². High *para* selectivity of SAPO-11 and CoAPO-11 is similar to that of ZSM-22¹³ and KZ-1¹⁴. Whereas ZSM-5 has nearly circular entry ports, the channels in the other two zeolites as well as in AlPO₄-11 are elliptical which gives rise to higher *para* selectivity.

Pellet *et al.*¹⁵ have briefly reported methylation of toluene on SAPO-11 and found very good *para* selectivity. They, however, did not report the details of product distribution. An important aspect is the formation of only 1,2,4-TMB on the *present* molecular sieves with total exclusion of the other isomers. TMB can be formed either by xylene disproportionation to toluene and TMB or by reaction between xylene and toluene to give TMB and benzene. Complete absence of benzene in the product rules out the latter possibility. Disproportionation of xylene would require a bulky biphenyl transition

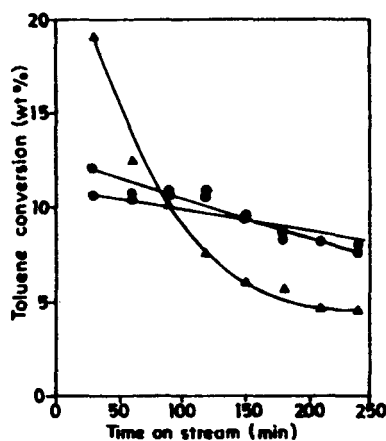


Fig. 5—Conversion vs time on stream plots for alkylation of toluene with methanol on various catalysts [—○— SAPO-11/1; —●— SAPO-11/2; —△— CoAPO-11].

Table 3—Alkylation of toluene with methanol : product distribution after 30 min
{Feed : toluene/CH₃OH : (2:1); H₂/HC (2:1); Temp. : 350°C; and WHSV : 2.6 h⁻¹}

Product (% wt)	AlPO ₄ -11	SAPO-11/1	SAPO-11/4	CoAPO-11
Toluene	99.2	89.4	87.3	81.0
Toluene converted	0.8	10.6	12.7	19.0
<i>p</i> -Xylene	0.56	6.28	6.02	7.37
<i>m</i> -Xylene	0.16	2.18	3.20	5.48
<i>o</i> -Xylene	0.10	1.10	1.85	2.66
1,2,4-TMB	—	1.0	1.63	3.51
<i>Para</i> selectivity*	2.15	1.92	1.19	0.91

**Para* selectivity = *p*-xylene/(*m*-xylene + *o*-xylene)

state. One can visualize three such transition states leading to 1,2,4-TMB, 1,2,3-TMB and 1,3,5-TMB respectively. It was shown by Martens *et al.*¹⁶ that the transition state leading to 1,2,4-TMB has the least space requirement. Formation of the other two transition states would require larger pores, intersecting channels or appropriately spaced regular side lobes in the channel. Since the 10-0 channels of $\text{AlPO}_4\text{-11}$ based structures are intersected only by small 4- and 6-0 channels, formation of the more bulky transition states can be ruled out. Hence, the absence of the other two TMB isomers can be explained as due to restricted transition state shape selectivity. All the three isomers of TMB are formed when¹⁷ toluene methylation is carried out on wide pore SAPO-5.

The present work thus indicates that substitution of Co^{2+} for aluminium leads to a comparatively strong acid sites, but they are still weaker than those present in the zeolites. In the presence of methanol, toluene undergoes alkylation on the presently studied catalysts without any disproportionation. Alkylation of toluene is highly *para* selective because of the elliptical 10-membered channels of the $\text{AlPO}_4\text{-11}$ framework.

Acknowledgement

Financial support from the DST, New Delhi, is gratefully acknowledged.

References

- 1 Meier WM & Olson DH, *Atlas of zeolite structure types*, 2nd Edn (Butterworths, London) 1987.
- 2 Lok BM, Messina CA, Patton RL, Gajek RT, Cannan TR & Flanigen EM, *J Am chem Soc*, 106 (1984) 6092.
- 3 Messina CA, Lok BM & Flanigen EM, *US Patent*, 4,554,143 (1985).
- 4 Long GN, Pellet RJ & Rabo JA, *US Patent*, 4,528,414 (1985).
- 5 Rabo JA, Pellet RJ, Cough PG & Shamsoum EG in *Zeolites as catalysts, sorbents and detergent builders*, edited by HG Karge and J Weitkamp (Elsevier, Amsterdam) 1989, 1.
- 6 Lok BM, Messina CA, Patton RL, Gajek RT, Cannan TR & Flanigen EM, *US Patent*, 4,440,871 (1984).
- 7 Shoonheydt RA, Vos R De, Pelgrims J & Leeman H in *Zeolites: Facts, figures and future*, edited by PA Jacobs & RA van Santeen, Part B (Elsevier, Amsterdam) 1989, 559.
- 8 Satyanarayana CVV & Chakrabarty DK, *Indian J Chem*, 30A (1991) 422.
- 9 Jahn E, Muller D & Becker K, *Zeolite*, 10 (1990) 151.
- 10 Martens JA, Grobet PJ & Jacobs PA, *J Catal*, 126 (1990) 299.
- 11 Kaeding WW, Chu C, Young LB, Weinstein B & Butter SA, *J Catal*, 67 (1981) 159.
- 12 Chen NY, Kaeding WW & Dwyer FG, *J Am chem Soc*, 101 (1979) 6783.
- 13 Kumar R, Rao GN & Ratnasamy P, in *Zeolites: Facts, figures and future*, edited by PA Jacobs & RA Van Santeen (Elsevier, Amsterdam) 1989, 1141.
- 14 Rane SJ & Chakrabarty DK, *Appl Catal*, 75 (1991) 281.
- 15 Pellet RJ, Long GN & Rabo JA, in *New developments in zeolite science and technology*, edited by Y Murakami, A Lijima & JW Wards (Elsevier, Amsterdam) 1986, 843.
- 16 Martens JA, Perez-Pariente J, Sastre E, Corma A & Jacobs PA, *Appl Catal*, 45 (1988) 85.
- 17 Das J & Chakrabarty DK (unpublished results).